

Chapter 7

Stellar models and stellar stability

In the previous chapters we have reviewed the most important physical processes taking place in stellar interiors, and we derived the differential equations that determine the structure and evolution of a star. By putting these ingredients together we can construct models of spherically symmetric stars. Because the complete set of equations is highly non-linear and time-dependent, their full solution requires a complicated numerical procedure. This is what is done in detailed stellar evolution codes, the results of which will be described in later chapters. We will not go into any detail about the numerical methods commonly used in such codes – for those interested, some of these details may be found in Chapter 24.2 of MAEDER or Chapter 11 of KIPPENHABHN.

The main purpose of this chapter is to briefly analyse the differential equations of stellar evolution and their boundary conditions, and to see how the full set of equations can be simplified in some cases to allow simple or approximate solutions – so-called *simple stellar models*. We also address the question of the stability of stars – whether the solutions to the equations yield a stable structure or not.

7.1 The differential equations of stellar evolution

Let us collect and summarize the differential equations for stellar structure and evolution that we have derived in the previous chapters, regarding m as the spatial variable, i.e. eqs. (2.6), (2.11), (5.4), (5.17) and (6.41):

$$\frac{\partial r}{\partial m} = \frac{1}{4\pi r^2 \rho} \quad (7.1)$$

$$\frac{\partial P}{\partial m} = -\frac{Gm}{4\pi r^4} - \frac{1}{4\pi r^2} \frac{\partial^2 r}{\partial t} \quad (7.2)$$

$$\frac{\partial l}{\partial m} = \epsilon_{\text{nuc}} - \epsilon_{\nu} - T \frac{\partial s}{\partial t} \quad (7.3)$$

$$\frac{\partial T}{\partial m} = -\frac{Gm}{4\pi r^4} \frac{T}{P} \nabla \quad \text{with} \quad \nabla = \begin{cases} \nabla_{\text{rad}} = \frac{3\kappa}{16\pi acG} \frac{lP}{mT^4} & \text{if } \nabla_{\text{rad}} \leq \nabla_{\text{ad}} \\ \nabla_{\text{ad}} + \Delta\nabla & \text{if } \nabla_{\text{rad}} > \nabla_{\text{ad}} \end{cases} \quad (7.4)$$

$$\frac{\partial X_i}{\partial t} = \frac{A_i m_u}{\rho} \left(-\sum_j (1 + \delta_{ij}) r_{ij} + \sum_{k,l} r_{kl,i} \right) \quad [+ \text{mixing terms}] \quad i = 1 \dots N \quad (7.5)$$

Note that eq. (7.2) is written in its general form, without pre-supposing hydrostatic equilibrium. In eq. (7.3) we have replaced $\partial u/\partial t - (P/\rho^2)\partial\rho/\partial t$ by $T\partial s/\partial t$, according to the combined first and second laws of thermodynamics. Eq. (7.4) is generalized to include both the cases of radiative and convective energy transport. The term $\Delta\nabla$ is the superadiabaticity of the temperature gradient that must follow from a theory of convection (in practice, the mixing length theory); for the interior one can take $\Delta\nabla = 0$ except in the outermost layers of a star. Finally, eq. (7.5) has been modified to add ‘mixing terms’ that describe the redistribution (homogenization) of composition in convective regions. There are N such equations, one for each nucleus (isotope) indicated by subscript i .

The set of equations above comprise $4 + N$ partial differential equations that should be solved simultaneously. Let us count the number of unknown variables. Making use of the physics discussed in previous chapters, the functions P , s , κ , ∇_{ad} , $\Delta\nabla$, ϵ_{nuc} , ϵ_{ν} and the reaction rates r_{ij} can all be expressed as functions of ρ , T and composition X_i . We are therefore left with $4 + N$ unknown variables (r , ρ , T , l and the X_i) so that we have a solvable system of equations.

The variables r , ρ , T , l and X_i appearing in the equations are all functions of two *independent* variables, m and t . We must therefore find a solution to the above set of equations on the interval $0 \leq m \leq M$ for $t > t_0$, assuming the evolution starts at time t_0 . Note that M generally also depends on t in the presence of mass loss. A solution therefore also requires specification of *boundary conditions* (at $m = 0$ and $m = M$) and of *initial conditions*, for example $X_i(m, t_0)$.

7.1.1 Timescales and initial conditions

Let us further analyse the equations. Three kinds of time derivatives appear:

- $\partial^2 r/\partial t^2$ in eq. (7.2), which describes hydrodynamical changes to the stellar structure. These occur on the dynamical timescale τ_{dyn} which as we have seen is very short. Thus we can normally assume hydrostatic equilibrium and $\partial^2 r/\partial t^2 = 0$, in which case eq. (7.2) reduces to the ordinary differential equation (2.13). Note that HE was explicitly assumed in eq. (7.4).
- $T\partial s/\partial t$ in eq. (7.3), which is often written as an additional energy generation term (eq. 5.5):

$$\epsilon_{\text{gr}} = -T \frac{\partial s}{\partial t} = -\frac{\partial u}{\partial t} + \frac{P}{\rho^2} \frac{\partial \rho}{\partial t}$$

It describes changes to the thermal structure of the star, which can result from contraction ($\epsilon_{\text{gr}} > 0$) or expansion ($\epsilon_{\text{gr}} < 0$) of the layers under consideration. Such changes occur on the thermal timescale τ_{KH} . If a star evolves on a much longer timescale than τ_{KH} then $\epsilon_{\text{gr}} \approx 0$ and the star is in thermal equilibrium. Then also eq. (7.3) reduces to an ordinary differential equation, eq. (5.7).

- $\partial X_i/\partial t$ in eqs. (7.5), describing changes in the composition. For the most abundant elements – the ones that affect the stellar structure – such changes normally occur on the longest, nuclear timescale τ_{nuc} .

Because normally $\tau_{\text{nuc}} \gg \tau_{\text{KH}} \gg \tau_{\text{dyn}}$, composition changes are usually very slow compared to the other time derivatives. In that case eqs. (7.5) decouple from the other four equations (7.1–7.4), which can be seen to describe the *stellar structure* for a given composition $X_i(m)$.

For a star in both HE and TE (also called ‘complete equilibrium’), the stellar structure equations (7.1–7.4) become a set of ordinary differential equations, independent of time. In that case it is sufficient to specify the initial composition profiles $X_i(m, t_0)$ as initial conditions. This is the case for so-called *zero-age main sequence* stars: the structure at the start of the main sequence depends only

on the initial composition, and is independent of the uncertain details of the star formation process, a very fortunate circumstance!

If a star starts out in HE, but not in TE, then the time derivative represented by ϵ_{gr} remains in the set of structure equations. One would then also have to specify the specific entropy profile $s(m, t_0)$ as an initial condition. This is the case if one considers pre-main sequence stars. Fortunately, as we shall see later, in this case there is also a simplifying circumstance: pre-main sequence stars start out as fully convective gas spheres. This means that their temperature and pressure stratification is nearly adiabatic, so that s can be taken as constant throughout the star. It then suffices to specify the initial entropy.

7.2 Boundary conditions

The boundary conditions for the differential equations of stellar evolution constitute an important part of the overall problem. Not all boundary conditions can be specified at one end of the interval $[0, M]$: some boundary conditions are set in the centre and others at the surface. This means that direct forward integration of the equations is not possible, and the influence of the boundary conditions on the solutions is not easy to foresee.

7.2.1 Central boundary conditions

At the centre ($m = 0$), both the density and the energy generation rate must remain finite. Therefore, both r and l must vanish in the centre:

$$m = 0 \quad : \quad r = 0 \quad \text{and} \quad l = 0. \quad (7.6)$$

However, nothing is known a priori about the central values of P and T . Therefore the remaining two boundary conditions must be specified at the surface rather than the centre.

It is possible to get some idea of the behaviour of the variables close to the centre by means of a Taylor expansion. Even though P_c and T_c are unknown, one can do this also for P and T , writing for example

$$P = P_c + m \left[\frac{dP}{dm} \right]_c + \frac{1}{2} m^2 \left[\frac{d^2 P}{dm^2} \right]_c + \dots$$

and making use of the stellar structure equations for dP/dm , etc, see Exercise 7.5.

7.2.2 Surface boundary conditions

At the surface ($m = M$, or $r = R$), the boundary conditions are generally much more complicated than at the centre. One may treat the surface boundary conditions at different levels of sophistication.

- The simplest option is to take $T = 0$ and $P = 0$ at the surface (the ‘zero’ boundary conditions). However, in reality T and P never become zero because the star is surrounded by an interstellar medium with very low, but finite density and temperature.
- A better option is to identify the surface with the *photosphere*, which is where the bulk of the radiation escapes and which corresponds with the visible surface of the star. The photospheric boundary conditions approximate the photosphere with a single surface at optical depth $\tau = \frac{2}{3}$. We can write

$$\tau_{\text{ph}} = \int_R^\infty \kappa \rho \, dr \approx \kappa_{\text{ph}} \int_R^\infty \rho \, dr, \quad (7.7)$$

where κ_{ph} is an average value of opacity over the atmosphere (all layers above the photosphere). If the atmosphere is geometrically thin we also have

$$\frac{dP}{dr} = -\frac{GM}{R^2}\rho \quad \Rightarrow \quad P(R) \approx \frac{GM}{R^2} \int_R^\infty \rho dr. \quad (7.8)$$

Since $\tau_{\text{ph}} = \frac{2}{3}$ and $T(R) \approx T_{\text{eff}}$ we can combine the above equations to write the photospheric boundary conditions as:

$$m = M(r = R) \quad : \quad P = \frac{2}{3} \frac{GM}{\kappa_{\text{ph}} R^2} \quad \text{and} \quad L = 4\pi R^2 \sigma T^4. \quad (7.9)$$

- The problem with the photospheric boundary conditions above is that the radiative diffusion approximation on which it is based breaks down when $\tau \lesssim$ a few. The best solution is therefore to fit a *detailed stellar atmosphere model* to an interior shell (at $\tau > \frac{2}{3}$) where the radiative diffusion approximation is still valid. This is a more complicated and time-consuming approach, and in many (but not all) practical situations the photospheric conditions are sufficient.

7.2.3 Effect of surface boundary conditions on stellar structure

It is instructive to look at the effect of the surface boundary conditions on the solution for the structure of the outer envelope of a star. Assuming complete (dynamical and thermal) equilibrium, the envelope contains only a small fraction of the mass and no energy sources. In that case $l = L$ and $m \approx M$. It is then better to take P , rather than m , as the independent variable describing depth within the envelope. We can write the equation for radiative energy transport as

$$\frac{dT}{dP} = \frac{T}{P} \nabla_{\text{rad}} = \frac{3}{16\pi acG} \frac{\kappa l}{m T^3} \approx \text{const} \cdot \frac{L}{M} \frac{\kappa}{T^3} \quad (7.10)$$

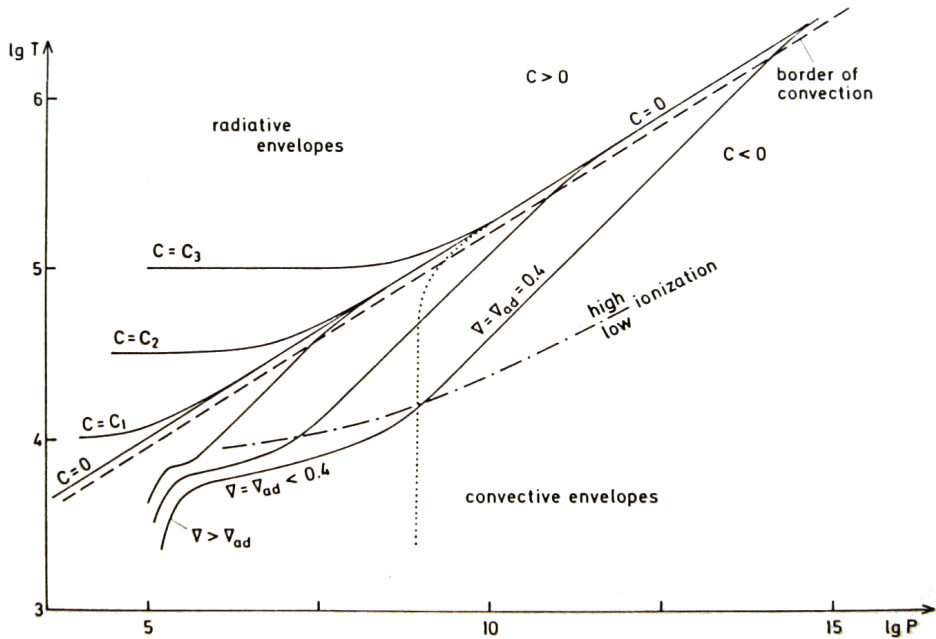


Figure 7.1. Schematic diagram of $\log T$ versus $\log P$ illustrating the different types of envelope structure solutions, as discussed in the text. Figure from KIPPENHAHN & WEIGERT.

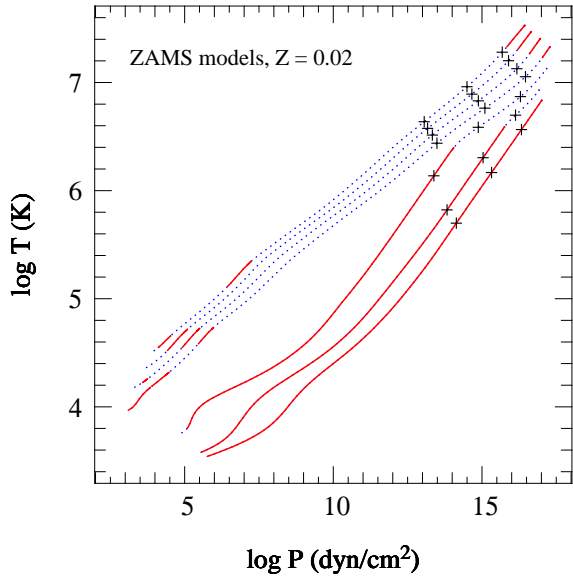


Figure 7.2. Structure of detailed stellar models on the zero-age main sequence in the $\log P$, $\log T$ diagram. Each curve is for a different mass, from top to bottom: $16 M_{\odot}$, $8 M_{\odot}$, $4 M_{\odot}$, $2 M_{\odot}$, $1 M_{\odot}$, $0.5 M_{\odot}$ and $0.25 M_{\odot}$. The + symbols on each curve indicate, for increasing P , the part of the envelope containing $0.01M$, $0.1M$ and $0.5M$ (so most of the T and P variation in the envelope occurs in the outer 1% of the mass). The dotted (blue) parts of each curve indicate radiative regions of the star, the solid (red) parts indicate convective regions.

Stars with $M \leq 1 M_{\odot}$ have low T_{eff} and therefore convective envelopes. The depth of the convective envelope increases strongly with decreasing surface temperature (and thus with decreasing mass); the $0.25 M_{\odot}$ star is completely convective. On the other hand, more massive stars have higher T_{eff} and mostly radiative envelopes, except for small convective layers near the surface caused by partial ionization.

We also approximate the opacity by a simple law, $\kappa = \kappa_0 P^a T^b$ (this can represent e.g. Kramers opacity, $a = 1$, $b = -4.5$; or electron scattering, $a = b = 0$). We can then integrate dT/dP to give

$$T^{4-b} = B(P^{1+a} + C) \quad (7.11)$$

where $B \propto L/M = \text{constant}$ and C is an integration constant, determined by the boundary conditions. For the Kramers opacity, which is a reasonable approximation for stellar envelopes of moderate temperatures, we find $T^{8.5} = B(P^2 + C)$.

The different possible solutions are characterized by the value of C , and the various possibilities are illustrated in Fig. 7.1. At large enough pressure, $P \gg \sqrt{C}$, all solutions approach $T \propto P^{2/8.5} \approx P^{0.235}$. This corresponds to an actual temperature gradient, $\nabla = d \log T / d \log P = 0.235 < \nabla_{\text{ad}} \approx 0.4$, which is consistent with the assumed radiative transport. There is a fundamental difference between solutions with $C \geq 0$ and $C < 0$, however.

Radiative envelopes correspond to solutions with $C \geq 0$. In the special case $C = 0$ the slope of the solution ∇ remains equal to 0.235 when $P, T \rightarrow 0$. This corresponds to the ‘zero’ boundary conditions discussed above. For $C > 0$ the solutions lie above the $C = 0$ line, and the slope decreases ($\nabla < 0.235$) as the surface is approached. This corresponds to more realistic, e.g. photospheric, boundary conditions with large enough T_{eff} , demonstrating that *stars with relatively hot photospheres have radiative envelopes*. In practice this is the case when $T_{\text{eff}} \gtrsim 9000$ K. Fig. 7.1 demonstrates that such envelope solutions quickly approach the ‘radiative zero’ structure, $C = 0$. This means that the envelope structure is insensitive to the assumed surface boundary conditions, and in practice the photospheric BC’s are sufficient.

Convective envelopes correspond to solutions with $C < 0$. In this case the solutions lie below the $C = 0$ line, and their slope increases as $\log P$ decreases. This is shown by the dotted line in Fig. 7.1. However, the assumption of radiative transport breaks down when $\nabla > \nabla_{\text{ad}} \approx 0.4$ and convection sets in. Therefore, *stars with cool photospheres have convective envelopes*, in practice when $T_{\text{eff}} \lesssim 9000$ K. The actual temperature stratification in the envelope is close to adiabatic, $\nabla = \nabla_{\text{ad}}$, until the surface is approached. Before this happens, however, partial ionization decreases ∇_{ad} below 0.4 and gives rise to a much shallower slope. Since the different

solution lie close together near the surface, but further apart in the interior, the structure of a convective envelope *is* sensitive to the surface boundary conditions. This means that the structure also depends on the uncertain details of near-surface convection (see Sec. 5.5). A small change or uncertainty in T_{eff} can have a large effect on the depth of the convective envelope! For small enough T_{eff} the whole star can become convective (leading to the Hayashi line in the H-R diagram, see Sect. 9.1.1).

The approximate description given here is borne out by detailed stellar structure calculations, as demonstrated in Fig. 7.2. Also note that if we assume electron scattering instead of Kramers opacity, the description remains qualitatively the same (the radiative zero solution then has $\nabla = 0.25$ instead of 0.235).

7.3 Equilibrium stellar models

For a star in both hydrostatic and thermal equilibrium, the four partial differential equations for stellar structure (eqs. 7.1–7.4) reduce to ordinary, time-independent differential equations. We can further simplify the situation somewhat, by ignoring possible neutrino losses (ϵ_ν) which are only important in very late stages of evolution, and ignoring the superadiabaticity of the temperature gradient in surface convection zones. We then arrive at the following set of structure equations that determine the stellar structure for a given composition profile $X_i(m)$:

$$\frac{dr}{dm} = \frac{1}{4\pi r^2 \rho} \quad (7.12)$$

$$\frac{dP}{dm} = -\frac{Gm}{4\pi r^4} \quad (7.13)$$

$$\frac{dl}{dm} = \epsilon_{\text{nuc}} \quad (7.14)$$

$$\frac{dT}{dm} = -\frac{Gm}{4\pi r^4} \frac{T}{P} \nabla \quad \text{with} \quad \nabla = \begin{cases} \nabla_{\text{rad}} = \frac{3\kappa}{16\pi acG} \frac{lP}{mT^4} & \text{if } \nabla_{\text{rad}} \leq \nabla_{\text{ad}} \\ \nabla_{\text{ad}} & \text{if } \nabla_{\text{rad}} > \nabla_{\text{ad}} \end{cases} \quad (7.15)$$

We note that the first two equations (7.12 and 7.13) describe the *mechanical structure* of the star, and the last two equations (7.14 and 7.15) describe the *thermal and energetic* structure. They are coupled to each other through the fact that, for a general equation of state, P is a function of both ρ and T .

Although simpler than the full set of evolution equations, this set still has no simple, analytic solutions. The reasons are that, first of all, the equations are very non-linear: e.g. $\epsilon_{\text{nuc}} \propto \rho T^\nu$ with $\nu \gg 1$, and κ is a complicated function of ρ and T . Secondly, the four differential equations are coupled and have to be solved simultaneously. Finally, the equations have boundary conditions at both ends, and thus require iteration to obtain a solution.

It is, however, possible to make additional simplifying assumptions so that under certain circumstances an analytic solution or a much simpler numerical solution is possible. We have already discussed one example of such a simplifying approach in Chapter 4, namely the case of *polytropic models* in which the pressure and density are related by an equation of the form

$$P = K \rho^\gamma.$$

Since in this case P does not depend on T , the mechanical structure of a stellar model can be computed in a simple way, independent of its thermal and energetic properties, by solving eqs. (7.12) and (7.13).

Another approach is to consider simple scaling relations between stellar models with different masses and radii, but all having the same (or a very similar) relative density distributions. If a detailed numerical solution can be computed for one particular star, these so-called *homology relations* can be used to find an approximate model for another star.

7.4 Homology relations

Solving the stellar structure equations almost always requires heavy numerical calculations, such as are applied in detailed stellar evolution codes. However, there is often a kind of similarity between the numerical solutions for different stars. These can be approximated by simple analytical scaling relations known as *homology relations*. In past chapters we have already applied simple scaling relations based on rough estimates of quantities appearing in the stellar structure equations. In this section we will put these relations on a firmer mathematical footing.

The requirements for the validity of homology are very restrictive, and hardly ever apply to realistic stellar models. However, homology relations can offer a rough but sometimes very helpful basis for interpreting the detailed numerical solutions. This applies to models for stars on the *main sequence* and to so-called *homologous contraction*.

Definition Compare two stellar models, with masses M_1 and M_2 and radii R_1 and R_2 . All interior quantities in star 1 are denoted by subscript '1' (e.g. the mass coordinate m_1), etc. Now consider so-called *homologous mass shells* which have the same relative mass coordinate, $x \equiv m/M$, i.e.

$$x = \frac{m_1}{M_1} = \frac{m_2}{M_2} \quad (7.16)$$

The two stellar models are said to be *homologous* if homologous mass shells within them are located at the same relative radii r/R , i.e.

$$\frac{r_1(x)}{R_1} = \frac{r_2(x)}{R_2} \quad \text{or} \quad \frac{r_1(x)}{r_2(x)} = \frac{R_1}{R_2} \quad (7.17)$$

for all x .

Comparing two homologous stars, the ratio of radii r_1/r_2 for homologous mass shells is constant. In other words, two homologous stars have *the same relative mass distribution*, and therefore (as we shall prove shortly) the same relative density distribution.

All models have to obey the stellar structure equations, so that the transition for one homologous model to another has consequences for all other variables. We start by analysing the first two structure equations.

- The first stellar structure equation (7.12) can be written for star 1 as

$$\frac{dr_1}{dx} = \frac{M_1}{4\pi r_1^2 \rho_1} \quad (7.18)$$

If the stars are homologous, then from eq. (7.17) we can substitute $r_1 = r_2 (R_1/R_2)$ and obtain

$$\frac{dr_2}{dx} = \frac{M_2}{4\pi r_2^2 \rho_2} \cdot \left[\frac{\rho_2}{\rho_1} \frac{M_1}{M_2} \left(\frac{R_2}{R_1} \right)^3 \right]. \quad (7.19)$$

We recognize the structure equation for the radius of star 2 (i.e. eq. 7.18 with subscript ‘1’ replaced by ‘2’), multiplied by the factor in square brackets on the right-hand side. This equation must hold generally, which is only the case if the factor in square brackets is equal to one for all values of x , that is if

$$\frac{\rho_2(x)}{\rho_1(x)} = \frac{M_2}{M_1} \left(\frac{R_2}{R_1} \right)^{-3}. \quad (7.20)$$

This must hold at any homologous mass shell, and therefore also at the centre of each star. The factor MR^{-3} is proportional to the average density $\bar{\rho}$, so that the density at any homologous shell scales with the central density, or with the average density:

$$\boxed{\rho(x) \propto \rho_c \propto \bar{\rho}} \quad (7.21)$$

Note that, therefore, any two polytropic models with the same index n are homologous to each other.

- We can apply a similar analysis to the second structure equation (7.13) for hydrostatic equilibrium. For star 1 we have

$$\frac{dP_1}{dx} = -\frac{GM_1^2 x}{4\pi r_1^4} \quad (7.22)$$

so that after substituting $r_1 = r_2 (R_1/R_2)$ we obtain

$$\frac{dP_1}{dx} = -\frac{GM_2^2 x}{4\pi r_2^4} \cdot \left[\left(\frac{M_1}{M_2} \right)^2 \left(\frac{R_2}{R_1} \right)^4 \right] = \frac{dP_2}{dx} \cdot \left[\left(\frac{M_1}{M_2} \right)^2 \left(\frac{R_2}{R_1} \right)^4 \right], \quad (7.23)$$

where the second equality follows because star 2 must also obey the hydrostatic equilibrium equation. Hence we have $dP_1/dx = C dP_2/dx$, with C equal to the (constant) factor in square brackets. Integrating we obtain $P_1(x) = C P_2(x) + B$, where the integration constant $B = 0$ because at the surface, $x \rightarrow 1$, for both stars $P \rightarrow 0$. Thus we obtain

$$\frac{P_2(x)}{P_1(x)} = \left(\frac{M_2}{M_1} \right)^2 \left(\frac{R_2}{R_1} \right)^{-4}, \quad (7.24)$$

at any homologous mass shell. Again this must include the centre, so that for all x :

$$\boxed{P(x) \propto P_c \propto \frac{M^2}{R^4}}. \quad (7.25)$$

The pressure required for hydrostatic equilibrium therefore scales with M^2/R^4 at any homologous shell. Note that we found the same scaling of the *central* pressure with M and R from our rough estimate in Sect. 2.2, and for polytropic models of the same index n .

We can combine eqs. (7.20) and (7.24) to show that two homologous stars must obey the following relation between pressure and density at homologous points,

$$\frac{P_2(x)}{P_1(x)} = \left(\frac{M_2}{M_1} \right)^{2/3} \left(\frac{\rho_2(x)}{\rho_1(x)} \right)^{4/3}, \quad (7.26)$$

or

$$P(x) \propto M^{2/3} \rho(x)^{4/3}. \quad (7.27)$$

7.4.1 Homology for radiative stars composed of ideal gas

In order to obtain simple homology relations from the other structure equations, we must make additional assumptions. We start by analysing eq. (7.15).

- First, let us assume the *ideal gas* equation of state,

$$P = \frac{\mathcal{R}}{\mu} \rho T.$$

Let us further assume that in each star the *composition is homogeneous*, so that μ is a constant for both stars, though not necessarily the same. We can then combine eqs. (7.20) and (7.24) to obtain a relation between the temperatures at homologous mass shells,

$$\frac{T_2(x)}{T_1(x)} = \frac{\mu_2}{\mu_1} \frac{M_2}{M_1} \left(\frac{R_2}{R_1} \right)^{-1} \quad \text{or} \quad \boxed{T(x) \propto T_c \propto \mu \frac{M}{R}} \quad (7.28)$$

- Second, we will assume the stars are in *radiative equilibrium*. We can then write eq. (7.15) as

$$\frac{d(T^4)}{dx} = - \frac{3M}{16\pi^2 ac} \frac{\kappa l}{r^4} \quad (7.29)$$

This contains two as yet unknown functions of x on the right-hand side, κ and l . We must therefore make additional assumptions about the opacity, which we can very roughly approximate by a power law,

$$\kappa = \kappa_0 \rho^a T^b. \quad (7.30)$$

For a Kramers opacity law, we would have $a = 1$ and $b = -3.5$. However, for simplicity let us assume a *constant opacity* throughout each star (but like μ , not necessarily the same for both stars). Then a similar reasoning as was held above for the pressure, allows us to transform eq. (7.29) into an expression for the ratio of luminosities at homologous points,

$$\left(\frac{T_2(x)}{T_1(x)} \right)^4 = \frac{l_2(x)}{l_1(x)} \frac{M_2}{M_1} \frac{\kappa_2}{\kappa_1} \left(\frac{R_2}{R_1} \right)^{-4} \quad \Rightarrow \quad \frac{l_2(x)}{l_1(x)} = \left(\frac{\mu_2}{\mu_1} \right)^4 \left(\frac{M_2}{M_1} \right)^3 \left(\frac{\kappa_2}{\kappa_1} \right)^{-1} \quad (7.31)$$

making use of eq. (7.28) to obtain the second expression. This relation also holds for the surface layer, i.e. for the total stellar luminosity L . Hence $l(x) \propto L$ and

$$\boxed{L \propto \frac{1}{\kappa} \mu^4 M^3} \quad (7.32)$$

This relation represents a *mass-luminosity relation* for a radiative, homogeneous star with constant opacity and ideal-gas pressure.

Note that we obtained a mass-luminosity relation (7.32) without making any assumption about the mode of energy generation (and indeed, without even having to assume thermal equilibrium, because we have not yet made use of eq. 7.14). We can thus expect a mass-luminosity relation to hold not only on the main-sequence, but for any star in radiative equilibrium. What this relation tells us is that the luminosity depends mainly on how efficiently energy can be transported by radiation: a higher

opacity gives rise to a smaller luminosity, because the nontransparent layers work like a blanket wrapped around the star. In practice, for a star in thermal equilibrium (e.g. on the main sequence) the power generated by nuclear reactions L_{nuc} adapts itself to the surface luminosity L , and thereby also the central temperature needed to make the nuclear reactions proceed at the rate dictated by L .

Note, however, that the simple mass-luminosity relation (7.32) depends on the assumption of constant opacity. If we assume a Kramers opacity law, the mass-luminosity also depends (weakly) on the radius. It is left as an exercise to show that, in this case

$$L \propto \frac{\mu^{7.5} M^{5.5}}{R^{0.5}}. \quad (7.33)$$

This means that if the opacity is not a constant, there is a weak dependence of the luminosity on the mode of energy generation, through the radius dependence (see Sec. 7.4.2).

7.4.2 Main sequence homology

For stars that are in thermal equilibrium we can make use of the last structure equation (7.14) to derive further homology relations for the radius as a function of mass. We then have to assume a specific form for the energy generation rate, say

$$\epsilon_{\text{nuc}} = \epsilon_0 \rho T^\nu \quad (7.34)$$

so that eq. (7.14) can be written as

$$\frac{dl}{dx} = \epsilon_0 M \rho T^\nu \quad (7.35)$$

By making use of the other homology relations, including the mass-luminosity relation eq. (7.32), we obtain for a homogeneous, radiative star with constant opacity and consisting of an ideal gas:

$$R \propto \mu^{(\nu-4)/(\nu+3)} M^{(\nu-1)/(\nu+3)} \quad (7.36)$$

The slope of this *mass-radius relation* therefore depends on ν , that is, on the mode of nuclear energy generation. For main-sequence stars, in which hydrogen fusion provides the energy source, there are two possibilities, see Table 7.1.

We can also obtain relations between the central temperature and central density and the mass of a star in thermal equilibrium, by combining the homology relations for the radius (7.36) with those for density and temperature (7.20 and 7.28):

$$\rho_c \propto \mu^{3(4-\nu)/(\nu+3)} M^{2(3-\nu)/(\nu+3)} \quad (7.37)$$

$$T_c \propto \mu^{7/(\nu+3)} M^{4/(\nu+3)} \quad (7.38)$$

Again, the result depends on the mode of energy generation through the value of ν . For main-sequence stars the possibilities are tabulated in Table 7.1.

The mass-luminosity and mass-radius relations (7.32) and (7.36) can be compared to the observed relations for main-sequence stars that were presented in Chapter 1, and to the results of detailed stellar structure calculations. This comparison is deferred to Chapter 9, where the main sequence is discussed in more detail.

Table 7.1. Homology relations for the radius, central temperature and central density of main-sequence stars

pp-chain	$\nu \approx 4$	$R \propto M^{0.43}$	$T_c \propto \mu M^{0.57}$	$\rho_c \propto M^{-0.3}$
CNO cycle	$\nu \approx 18$	$R \propto \mu^{2/3} M^{0.81}$	$T_c \propto \mu^{1/3} M^{0.19}$	$\rho_c \propto \mu^{-2} M^{-1.4}$

7.4.3 Homologous contraction

We have seen in Chapter 2 that, as a consequence of the virial theorem, a star without internal energy sources must contract under the influence of its own self-gravity. Suppose that this contraction takes place homologously. According to eq. (7.17) each mass shell inside the star then maintains the same relative radius r/R . Writing $\dot{r} = \partial r / \partial t$, etc., this means that

$$\frac{\dot{r}(m)}{r(m)} = \frac{\dot{R}}{R}.$$

Since in this case we compare homologous models with the same mass M , we can replace x by the mass coordinate m . For the change in density we obtain from eq. (7.20) that

$$\frac{\dot{\rho}(m)}{\rho(m)} = -3 \frac{\dot{R}}{R}, \quad (7.39)$$

and if the contraction occurs *quasi-statically*, i.e. slow enough to maintain HE, then the change in pressure follows from eq. (7.24),

$$\frac{\dot{P}(m)}{P(m)} = -4 \frac{\dot{R}}{R} = \frac{4}{3} \frac{\dot{\rho}(m)}{\rho(m)}. \quad (7.40)$$

To obtain the change in temperature for a homologously contracting star, we have to consider the equation of state. Writing the equation of state in its general, differential form eq. (3.48) we can eliminate \dot{P}/P to get

$$\frac{\dot{T}}{T} = \frac{1}{\chi_T} \left(\frac{4}{3} - \chi_\rho \right) \frac{\dot{\rho}}{\rho} = \frac{1}{\chi_T} (3\chi_\rho - 4) \frac{\dot{R}}{R}. \quad (7.41)$$

Hence the temperature increases as a result of contraction as long as $\chi_\rho < \frac{4}{3}$. For an ideal gas, with $\chi_\rho = 1$, the temperature indeed increases upon contraction, in accordance with our (qualitative) conclusion from the virial theorem. Quantitatively,

$$\frac{\dot{T}}{T} = \frac{1}{3} \frac{\dot{\rho}}{\rho}.$$

However, for a degenerate electron gas with $\chi_\rho = \frac{5}{3}$ eq. (7.41) shows that the temperature decreases, in other words a degenerate gas sphere will *cool* upon contraction. The full consequences of this important result will be explored in Chapter 8.

7.5 Stellar stability

We have so far considered stars in both hydrostatic and thermal equilibrium. But an important question that remains to be answered is whether these equilibria are *stable*. From the fact that stars can preserve their properties for very long periods of time, we can guess that this is indeed the case. But in order to answer the question of stability, and find out under what circumstances stars may become unstable, we must test what happens when the equilibrium situation is perturbed: will the perturbation be quenched (stable situation) or will it grow (unstable situation). Since there are two kinds of equilibria, we have to consider two kinds of stability:

- dynamical stability: what happens when hydrostatic equilibrium is perturbed?
- thermal (secular) stability: what happens when the thermal equilibrium situation is perturbed?

7.5.1 Dynamical stability of stars

The question of dynamical stability relates to the response of a certain part of a star to a perturbation of the balance of forces that act on it: in other words, a perturbation of hydrostatic equilibrium. We already treated the case of dynamical stability to *local* perturbations in Sec. 5.5.1, and saw that in this case instability gives rise to *convection*. In this section we look at the global stability of concentric layers within a star to radial perturbations, i.e. compression or expansion. A rigorous treatment of this problem is very complicated, so we will only look at a very simplified example to illustrate the principles.

Suppose a star in hydrostatic equilibrium is compressed on a short timescale, $\tau \ll \tau_{\text{KH}}$, so that the compression can be considered as adiabatic. Furthermore suppose that the compression occurs *homologously*, such that its radius decreases from R to R' . Then the density at any layer in the star becomes

$$\rho \rightarrow \rho' = \rho \left(\frac{R'}{R} \right)^{-3}$$

and the new pressure after compression becomes P' , given by the adiabatic relation

$$\frac{P'}{P} = \left(\frac{\rho'}{\rho} \right)^{\gamma_{\text{ad}}} = \left(\frac{R'}{R} \right)^{-3\gamma_{\text{ad}}}.$$

The pressure required for HE after homologous contraction is

$$\left(\frac{P'}{P} \right)_{\text{HE}} = \left(\frac{\rho'}{\rho} \right)^{4/3} = \left(\frac{R'}{R} \right)^{-4}$$

Therefore, if $\gamma_{\text{ad}} > \frac{4}{3}$ then $P' > P'_{\text{HE}}$ and the excess pressure leads to re-expansion (on the dynamical timescale τ_{dyn}) so that HE is restored. If, however, $\gamma_{\text{ad}} < \frac{4}{3}$ then $P' < P'_{\text{HE}}$ and the increase of pressure is not sufficient to restore HE. The compression will therefore reinforce itself, and the situation is unstable on the dynamical timescale. We have thus obtained a criterion for *dynamical stability*:

$$\boxed{\gamma_{\text{ad}} > \frac{4}{3}} \quad (7.42)$$

It can be shown rigorously that a star that has $\gamma_{\text{ad}} > \frac{4}{3}$ everywhere is dynamically stable, and if $\gamma_{\text{ad}} = \frac{4}{3}$ it is neutrally stable. However, the situation when $\gamma_{\text{ad}} < \frac{4}{3}$ in some part of the star requires further investigation. It turns out that global dynamical instability is obtained when the integral

$$\int \left(\gamma_{\text{ad}} - \frac{4}{3} \right) \frac{P}{\rho} dm \quad (7.43)$$

over the whole star is negative. Therefore if $\gamma_{\text{ad}} < \frac{4}{3}$ in a sufficiently large core, where P/ρ is high, the star becomes unstable. However if $\gamma_{\text{ad}} < \frac{4}{3}$ in the outer layers where P/ρ is small, the star as a whole need not become unstable.

Cases of dynamical instability

Stars dominated by an ideal gas or by non-relativistic degenerate electrons have $\gamma_{\text{ad}} = \frac{5}{3}$ and are therefore dynamically stable. However, we have seen that for relativistic particles $\gamma_{\text{ad}} \rightarrow \frac{4}{3}$ and stars dominated by such particles tend towards a neutrally stable state. A small disturbance of such a star could either lead to a collapse or an explosion. This is the case if *radiation pressure* dominates (at high T and low ρ), or the pressure of relativistically degenerate electrons (at very high ρ).

A process that can lead to $\gamma_{\text{ad}} < \frac{4}{3}$ is *partial ionization* (e.g. $\text{H} \leftrightarrow \text{H}^+ + \text{e}^-$), as we have seen in Sect. 3.5. Since this normally occurs in the very outer layers, where P/ρ is small, it does not lead to overall dynamical instability of the star. However, partial ionization is connected to driving oscillations in some kinds of star.

At very high temperatures two other processes can occur that have a similar effect to ionization. These are *pair creation* ($\gamma + \gamma \leftrightarrow \text{e}^+ + \text{e}^-$, see Sect. 3.6.2) and *photo-disintegration* of nuclei (e.g. $\gamma + \text{Fe} \leftrightarrow \alpha$). These processes, that may occur in massive stars in late stages of evolution, also lead to $\gamma_{\text{ad}} < \frac{4}{3}$ but now in the core of the star. These processes can lead to a stellar explosion or collapse (see Chapter 13).

7.5.2 Secular stability of stars

The question of thermal or *secular* stability, i.e. the stability of thermal equilibrium, is intimately linked to the virial theorem. In the case of an ideal gas the virial theorem (Sect. 2.3) tells us that the total energy of a star is

$$E_{\text{tot}} = -E_{\text{int}} = \frac{1}{2}E_{\text{gr}}, \quad (7.44)$$

which is negative: the star is bound. The rate of change of the total energy is given by the difference between the rate of nuclear energy generation in the deep interior and the rate of energy loss in the form of radiation from the surface:

$$\dot{E}_{\text{tot}} = L_{\text{nuc}} - L \quad (7.45)$$

In a state of thermal equilibrium, $L = L_{\text{nuc}}$ and E_{tot} remains constant. Consider now a small perturbation of this situation, for instance $L_{\text{nuc}} > L$ because of a small temperature fluctuation. This leads to an increase of the total energy, $\delta E_{\text{tot}} > 0$, and since the total energy is negative, its absolute value becomes smaller. The virial theorem, eq. (7.44), then tells us that (1) $\delta E_{\text{gr}} > 0$, in other words the star will expand ($\delta \rho < 0$), and (2) $\delta E_{\text{int}} < 0$, meaning that the overall temperature will decrease ($\delta T < 0$). Since the nuclear energy generation rate $\epsilon_{\text{nuc}} \propto \rho T^\nu$ depends on positive powers of ρ and especially T , the total nuclear energy generation will decrease: $\delta L_{\text{nuc}} < 0$. Eq. (7.45) shows that the perturbation to E_{tot} will be quenched and the state of thermal equilibrium will be restored.

The secular stability of nuclear burning thus depends on the *negative heat capacity* of stars composed of ideal gas: the property that an increase of the total energy content leads to a decrease of the temperature. This property provides a *thermostat* that keeps the temperature nearly constant and keeps stars in a stable state of thermal equilibrium for such long time scales.

We can generalise this to the case of stars with appreciable radiation pressure. For a mixture of ideal gas and radiation we can write, with the help of eqs. (3.11) and (3.12),

$$\frac{P}{\rho} = \frac{P_{\text{gas}}}{\rho} + \frac{P_{\text{rad}}}{\rho} = \frac{2}{3}u_{\text{gas}} + \frac{1}{3}u_{\text{rad}}. \quad (7.46)$$

Applying the virial theorem in its general form, eq. (2.24), this yields

$$2E_{\text{int,gas}} + E_{\text{int,rad}} = -E_{\text{gr}} \quad (7.47)$$

and the total energy becomes

$$E_{\text{tot}} = -E_{\text{int,gas}} = \frac{1}{2}(E_{\text{gr}} + E_{\text{int,rad}}). \quad (7.48)$$

The radiation pressure thus has the effect of reducing the effective gravitational potential energy. If $\beta = P_{\text{gas}}/P$ is constant throughout the star, then eq. (7.48) becomes

$$E_{\text{tot}} = \frac{1}{2}\beta E_{\text{gr}} \quad (7.49)$$

This is negative as long as $\beta > 0$. The analysis of thermal stability is analogous to the case of an ideal gas treated above, and we see that stars in which radiation pressure is important, but not dominant, are still secularly stable. However, if $\beta \rightarrow 0$ then the thermostatic effect no longer works.

Thermal instability of degenerate gases

In the case of a degenerate electron gas, the pressure and the internal energy are independent of the temperature (Sec. 3.3.5). The mechanical structure of an electron-degenerate star – or the degenerate core of an evolved star – is therefore independent of the thermal-energetic structure (Sec. 7.3). If the same perturbation $L_{\text{nuc}} > L$ discussed above is applied to a degenerate gas, the resulting energy input will have no effect on the electron pressure and on the stellar structure. Therefore there will be no expansion and cooling. Instead, there will be a temperature *increase* because the ionized atomic nuclei still behave as an ideal gas, and the energy input will increase their thermal motions. Thus the effect of the perturbation will be $\delta T > 0$, while $\delta \rho \approx 0$.

Because of the strong sensitivity of the nuclear energy generation rate to T , the perturbation will now lead to an increase of L_{nuc} , and thermal equilibrium will not be restored. Instead, the temperature will continue to rise as a result of the increased nuclear energy release, which in turn leads to further enhancement of the energy generation. This instability is called a *thermonuclear runaway*, and it occurs whenever nuclear reactions ignite in a degenerate gas. In some cases it can lead to the explosion of the star, although a catastrophic outcome can often be avoided when the gas eventually becomes sufficiently hot to behave as an ideal gas, for which the stabilizing thermostat operates. This can be seen from eq. (7.41), valid in the case of homologous expansion, which we can write as

$$\frac{\delta T}{T} = \frac{1}{\chi_T} \left(\frac{4}{3} - \chi_\rho \right) \frac{\delta \rho}{\rho}. \quad (7.50)$$

As soon as the gas is heated enough that it is no longer completely degenerate, $\chi_T > 0$ and some expansion will occur ($\delta \rho < 0$), while χ_ρ decreases below $\frac{5}{3}$. From eq. (7.50) we see that when χ_ρ drops below the critical value of $\frac{4}{3}$, δT changes sign and becomes negative upon further expansion.

We shall encounter several examples of thermonuclear runaways in future chapters. The most common occurrence is the ignition of helium fusion in stars with masses below about $2 M_\odot$ – this phenomenon is called the *helium flash*. Thermonuclear runaways also occur when hydrogen gas accumulates on the surface of a white dwarf, giving rise to so-called *nova outbursts*.

The thin shell instability

In evolved stars, nuclear burning can take place in a shell around an inert core. If such a burning shell is sufficiently thin the burning may become thermally unstable, even under ideal-gas conditions. We can make this plausible by considering a shell with mass Δm inside a star with radius R , located between a fixed inner boundary at r_0 and outer boundary at r , so that its thickness is $d = r - r_0 \ll R$. If the shell is in thermal equilibrium, the rate of nuclear energy generation equals the net rate of heat flowing out of the shell (eq. 7.14). A perturbation by which the energy generation rate exceeds the rate of heat flow leads to expansion of the shell, pushing the layers above it outward ($\delta r > 0$). This leads to a decreased pressure, which in hydrostatic equilibrium is given by eq. (7.40),

$$\frac{\delta P}{P} = -4 \frac{\delta r}{r}. \quad (7.51)$$

The mass of the shell is $\Delta m = 4\pi r_0^2 \rho d$, and therefore the density varies with the thickness of the shell as

$$\frac{\delta \rho}{\rho} = -\frac{\delta d}{d} = -\frac{\delta r}{r} \frac{r}{d}. \quad (7.52)$$

Eliminating $\delta r/r$ from the above equations yields a relation between the changes in pressure and density,

$$\frac{\delta P}{P} = 4 \frac{d}{r} \frac{\delta \rho}{\rho}. \quad (7.53)$$

Combining with the equation of state in its general, differential form eq. (3.48) we can eliminate $\delta P/P$ to obtain the resulting change in temperature,

$$\frac{\delta T}{T} = \frac{1}{\chi_T} \left(4 \frac{d}{r} - \chi_\rho \right) \frac{\delta \rho}{\rho}. \quad (7.54)$$

The shell is thermally stable as long as expansion results in a drop in temperature, i.e. when

$$4 \frac{d}{r} > \chi_\rho \quad (7.55)$$

since $\chi_T > 0$. Thus, for a sufficiently thin shell a thermal instability will develop. (In the case of an ideal gas, the condition 7.55 gives $d/r > 0.25$, but this is only very approximate.) If the shell is very thin, the expansion does not lead to a sufficient decrease in pressure to yield a temperature drop, even in the case of an ideal gas. This may lead to a runaway situation, analogous to the case of a degenerate gas. The thermal instability of thin burning shells is important during late stages of evolution of stars up to about $8 M_\odot$, during the *asymptotic giant branch*.

Suggestions for further reading

The contents of this chapter are also (partly) covered by Chapter 24 of MAEDER, where the question of stability is considered in Section 3.5. A more complete coverage of the material is given in Chapters 9, 10, 19, 20 and 25 of KIPPENHAHN.

Exercises

7.1 General understanding of the stellar evolution equations

The differential equations (7.1–7.5) describe, for a certain location in the star at mass coordinate m , the behaviour of and relations between radius coordinate r , the pressure P , the temperature T , the luminosity l and the mass fractions X_i of the various elements i .

- Which of these equations describe the mechanical structure, which describe the thermal-energetic structure and which describe the composition?
- What does ∇ represent? Which two cases do we distinguish?
- How does the set of equations simplify when we assume hydrostatic equilibrium (HE)? If we assume HE, which equation introduces a time dependence? Which physical effect does this time dependence represent?
- What do the terms ϵ_{nuc} and $T \partial s / \partial t$ represent?
- How does the set of equations simplify if we also assume thermal equilibrium (TE)? Which equation introduces a time dependence in TE?
- Equation (7.5) describes the changes in the composition. In principle we need one equation for every possible isotope. In most stellar evolution codes, the nuclear network is simplified. This reduces the number of differential equations and therefore increases speed of stellar evolution codes. The STARS code behind *Window to the Stars* only takes into account seven isotopes. Which do you think are most important?

7.2 Dynamical Stability

- Show that for a star in hydrostatic equilibrium ($dP/dm = -Gm/(4\pi r^4)$) the pressure scales with density as $P \propto \rho^{4/3}$.
- If $\gamma_{\text{ad}} < 4/3$ a star becomes dynamically unstable. Explain why.
- In what type of stars $\gamma_{\text{ad}} \approx 4/3$?
- What is the effect of partial ionization (for example $\text{H} \rightleftharpoons \text{H}^+ + \text{e}^-$) on γ_{ad} ? So what is the effect of ionization on the stability of a star?
- Pair creation* and *photo-disintegration* of Fe have a similar effect on γ_{ad} . In what type of stars (and in what phase of their evolution) do these processes play a role?

7.3 Mass radius relation for degenerate stars

- Derive how the radius scales with mass for stars composed of a *non-relativistic completely degenerate* electron gas. Assume that the central density $\rho_c = a\bar{\rho}$ and that the central pressure $P_c = bGM^2/R^4$, where $\bar{\rho}$ is the mean density, and a and b depend only on the density distribution inside the star.
- Do the same for an *extremely relativistic degenerate* electron gas.
- The electrons in a not too massive white dwarf behave like a completely degenerate non-relativistic gas. Many of these white dwarfs are found in binary systems. Describe qualitatively what happens if the white dwarf accretes material from the companion star.

7.4 Main-sequence homology relations

We speak of two *homologous stars* when they have the same density distribution. To some extent main sequence stars can be considered as stars with a similar density distribution.

- You already derived some scaling relations for main sequence stars from observations in the first set of exercises: the mass-luminosity relation and the mass-radius relation. Over which mass range were these simple relations valid?
- During the practicum you plotted the density distribution of main sequence stars of different masses. For which mass ranges did you find that the stars had approximately the same density distribution.
- Compare the L - M relation derived from observational data with the L - M relation derived from homology, eq. (7.32). What could cause the difference? (Which assumptions may not be valid?)
- Show that, if we replace the assumption of a constant opacity with a Kramers opacity law, the mass-luminosity-radius relation becomes eq. (7.33),

$$L \propto \frac{\mu^{7.5} M^{5.5}}{R^{0.5}}.$$

- Substitute a suitable mass-radius relation and compare the result of (d) with the observational data in Fig. 1.3. For which stars is the Kramers-based L - M relation the best approximation? Can you explain why? What happens at lower and higher masses, respectively?

7.5 Central behaviour of the stellar structure equations

- Rewrite the four structure equations in terms of d/dr .
- Find how the following quantities behave in the neighbourhood of the stellar center:
 - the mass $m(r)$,
 - the luminosity $l(r)$,
 - the pressure $P(r)$,
 - the temperature $T(r)$.

Chapter 8

Schematic stellar evolution – consequences of the virial theorem

8.1 Evolution of the stellar centre

We will consider the schematic evolution of a star, as seen from its centre. The centre is the point with the highest pressure and density, and (usually) the highest temperature, where nuclear burning proceeds fastest. Therefore, the centre is the most evolved part of the star, and it sets the pace of evolution, with the outer layers lagging behind.

The stellar centre is characterized by the central density ρ_c , pressure P_c and temperature T_c and the composition (usually expressed in terms of μ and/or μ_e). These quantities are related by the equation of state (EOS). We can thus represent the evolution of a star by an evolutionary track in the (P_c, ρ_c) diagram or the (T_c, ρ_c) diagram.

8.1.1 Hydrostatic equilibrium and the P_c - ρ_c relation

Consider a star in hydrostatic equilibrium (HE), for which we can estimate how the central pressure scales with mass and radius from the homology relations (Sec. 7.4). For a star that expands or contracts homologously, we can apply eq. (7.26) to the central pressure and central density to yield

$$P_c = C \cdot GM^{2/3} \rho_c^{4/3} \quad (8.1)$$

where C is a constant. This is a fundamental relation for stars in HE: *in a star of mass M that expands or contracts homologously, the central pressure varies as central density to the power $\frac{4}{3}$* . The value of the constant C depends on the density distribution in the star. Note that we found the same relation for polytropic stellar models in Chapter 4, eq. (4.18), where $C = C_n$ depends on the polytropic index. However, the dependence on n , and hence on the density distribution, is only very weak. For polytropic models with index $n = 1.5 - 3$, a range that encompasses most actual stars, C varies between 0.48 and 0.36. Hence relation (8.1) is reasonably accurate, even if the contraction is not exactly homologous. In other words: for a star of a certain mass, the central pressure is almost uniquely determined by the central density.

Note that we have obtained this relation without considering the EOS. Therefore (8.1) defines a *universal relation for stars in HE* that is independent of the equation of state. It expresses the fact that a star that contracts quasi-statically must achieve a higher internal pressure to remain in hydrostatic equilibrium. Eq. (8.1) therefore defines an *evolution track* of a slowly contracting (or expanding) star in the P_c - ρ_c plane.

8.1.2 The equation of state and evolution in the P_c - ρ_c plane

By considering the EOS we can also derive the evolution of the central temperature. This is obviously crucial for the evolutionary fate of a star because e.g. nuclear burning requires T_c to reach certain (high) values. We start by considering lines of constant T , *isotherms*, in the (P, ρ) plane.

We have encountered various regimes for the EOS in Chapter 3:

- Radiation dominated: $P = \frac{1}{3}aT^4$. Hence an isotherm in this region is also a line of constant P .
- (Classical) ideal gas: $P = \frac{\mathcal{R}}{\mu}\rho T$. Hence an isotherm has $P \propto \rho$.
- Non-relativistic electron degeneracy: $P = K_{NR}(\rho/\mu_e)^{5/3}$ (eq. 3.35). This is independent of temperature. More accurately: the complete degeneracy implied by this relation is only achieved when $T \rightarrow 0$, so this is in fact the isotherm for $T = 0$ (and not too high densities).
- Extremely relativistic electron degeneracy: $P = K_{ER}(\rho/\mu_e)^{4/3}$ (eq. 3.37). This is the isotherm for $T = 0$ and very high ρ .

Figure 8.1 shows various isotherms schematically in the $\log \rho$ - $\log P$ plane. Where radiation pressure dominates (low ρ) the isotherms are horizontal and where ideal-gas pressure dominates they have a slope = 1. The isotherm for $T = 0$, corresponding to complete electron degeneracy, has slope of $\frac{5}{3}$ at relatively low density and a shallower slope of $\frac{4}{3}$ at high density. The region to the right and below the $T = 0$ line is forbidden by the Pauli exclusion principle, since electrons are fermions.

The dashed lines are schematic evolution tracks for stars of different masses M_1 and M_2 . According to eq. (8.1) they have a slope of $\frac{4}{3}$ and the track for a larger mass lies at a higher pressure than that for a smaller mass.

Several important conclusions can be drawn from this diagram:

- As long as the gas is ideal, contraction (increasing ρ_c) leads to a higher T_c , because the slope of the evolution track is steeper than that of ideal-gas isotherms: the evolution track crosses isotherms of higher and higher temperature.

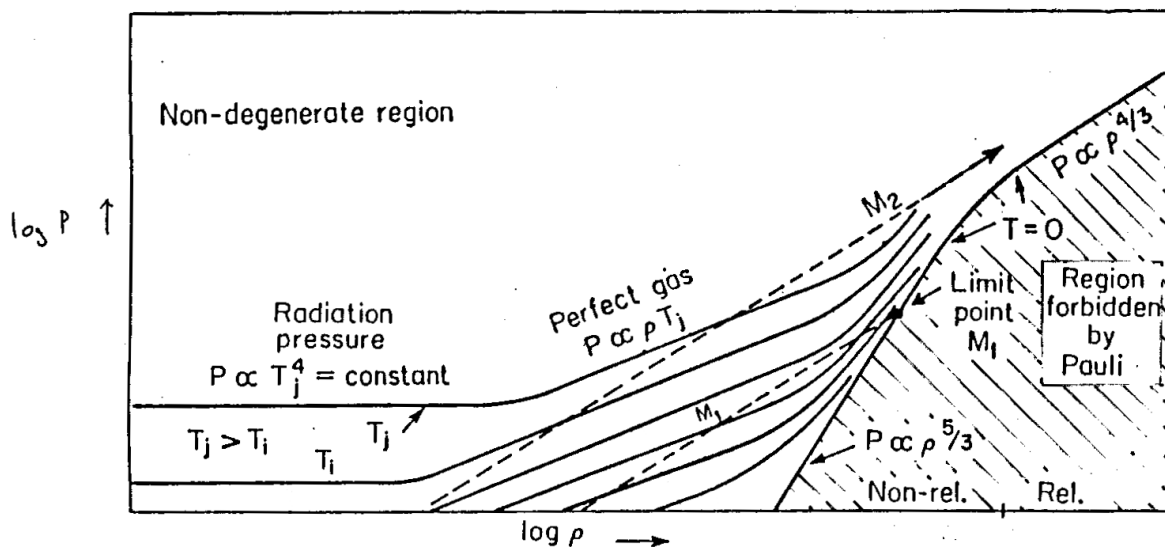


Figure 8.1. Schematic evolution in the $\log \rho$ - $\log P$ plane. Solid lines are isotherms in the equation of state; the dashed lines indicate two evolution tracks of different mass, which have a slope of $\frac{4}{3}$. See the text for an explanation.

Note that this is consistent with what we have already concluded from the virial theorem for an ideal gas: $E_{\text{in}} = -\frac{1}{2}E_{\text{gr}}$. Contraction (decreasing E_{gr} , i.e. increasing $-E_{\text{gr}}$) leads to increasing internal (thermal) energy of the gas, i.e. to heating of the stellar gas!

- Tracks for masses lower than some critical value M_{crit} , e.g. the track labeled M_1 , eventually run into the line for complete electron degeneracy because this has a steeper slope. Hence for stars with $M < M_{\text{crit}}$ there exist a maximum achievable central density and pressure, $\rho_{\text{c,max}}$ and $P_{\text{c,max}}$, which define the endpoint of their evolution. This endpoint is a completely degenerate state, i.e. a white dwarf, where the pressure needed to balance gravity comes from electrons filling the lowest possible quantum states.

Because complete degeneracy corresponds to $T = 0$, it follows that the evolution track must intersect each isotherm twice. In other words, stars with $M < M_{\text{crit}}$ also reach a maximum temperature $T_{\text{c,max}}$, at the point where degeneracy starts to dominate the pressure, after which further contraction leads to decreasing T_{c} . $\rho_{\text{c,max}}$, $P_{\text{c,max}}$ and $T_{\text{c,max}}$ all depend on M and increase with mass.

- Tracks for masses larger than M_{crit} , e.g. the one labeled M_2 , miss the completely degenerate region of the EOS, because at high ρ this has the same slope as the evolution track. This change in slope is owing to the electrons becoming relativistic and as their velocity cannot exceed c , they exert less pressure than if there were no limit to their velocity. Hence, electron degeneracy is not sufficient to counteract gravity, and a star with $M > M_{\text{crit}}$ must keep on contracting and getting hotter indefinitely – up to the point where the assumptions we have made break down, e.g. when ρ becomes so high that the protons inside the nuclei capture free electrons and a neutron gas is formed, which can also become degenerate.

Hence the evolution of stars with $M > M_{\text{crit}}$ is qualitatively different from that of stars with $M < M_{\text{crit}}$. This critical mass is none other than the *Chandrasekhar mass* that we have already encountered in Chapter 4 (eq. 4.22)

$$M_{\text{Ch}} = \frac{5.836}{\mu_e^2} M_{\odot}. \quad (8.2)$$

It is the unique mass of a completely degenerate and extremely relativistic gas sphere. A star with $M \geq M_{\text{Ch}}$ must collapse under its own gravity, but the electrons become extremely relativistic – and, if M is equal to or not much larger than M_{Ch} , also degenerate – in the process.

8.1.3 Evolution in the $T_{\text{c}}-\rho_{\text{c}}$ plane

We now consider how the stellar centre evolves in the $T_{\text{c}}, \rho_{\text{c}}$ diagram. First we divide the T, ρ plane into regions where different processes dominate the EOS, see Sec. 3.3.7 and Fig. 3.4, reproduced in Fig. 8.2a.

For a slowly contracting star in hydrostatic equilibrium equation (8.1) implies that, as long as the gas behaves like a classical ideal gas:

$$\frac{\mathcal{R}}{\mu} T_{\text{c}} \rho_{\text{c}} = C G M^{2/3} \rho_{\text{c}}^{4/3} \quad \rightarrow \quad T_{\text{c}} = \frac{C G}{\mathcal{R}} \mu M^{2/3} \rho_{\text{c}}^{1/3} \quad (8.3)$$

(Compare to Sec. 7.4.3.) This defines an evolution track in the $\log T, \log \rho$ plane with slope $\frac{1}{3}$. Stars with different mass evolve along tracks that lie parallel to each other, those with larger M lying at higher T_{c} and lower ρ_{c} . Tracks for larger mass therefore lie closer to the region where radiation

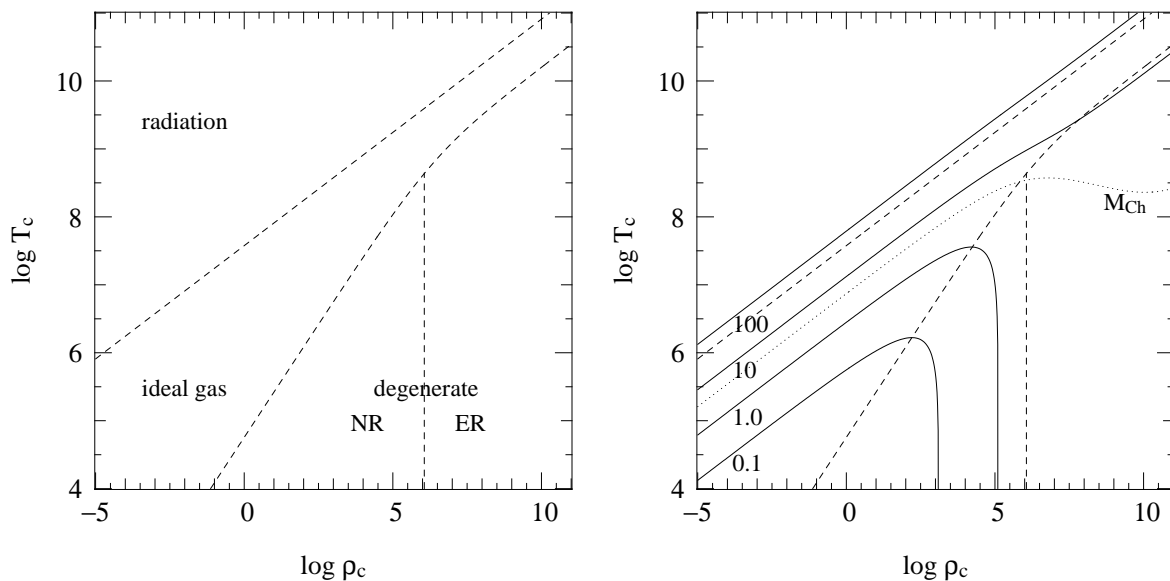


Figure 8.2. The equation of state in the $\log T_c - \log \rho_c$ plane (left panel), with approximate boundaries between regions where radiation pressure, ideal gas pressure, non-relativistic electron degeneracy and extremely relativistic electron degeneracy dominate, for a composition of $X = 0.7$ and $Z = 0.02$. In the right panel, schematic evolution tracks for contracting stars of $0.1 - 100 M_\odot$ have been added.

pressure is important: *the larger the mass of a star, the more important is the radiation pressure*. Furthermore, the relative importance of radiation pressure does not change as a star contracts, because the track runs parallel to the boundary between ideal gas and radiation pressure.¹

As the density increases, stars with $M < M_{Ch}$ approach the region where non-relativistic electron degeneracy dominates, because the boundary between ideal gas and NR degeneracy has a steeper slope than the evolution track. Inside this region, equating relation (8.1) to the NR degenerate pressure gives:

$$K_{NR} \frac{\rho_c^{1/3}}{\mu_e^{5/3}} = C G M^{2/3} \quad \rightarrow \quad \boxed{\rho_c = \left(\frac{C G}{K_{NR}} \right)^3 \mu_e^5 M^2} \quad (8.4)$$

When degeneracy dominates the track becomes independent of T_c , and the star moves down along a track of constant ρ_c . This is the $\rho_{c,max}$ we found from the P_c, ρ_c diagram. The larger the mass, the higher this density. (When the electrons become relativistic at $\rho_c \gtrsim 10^6 \text{ g/cm}^3$, the pressure increases less steeply with density so that the central density for a degenerate star of mass M is in fact larger than given by eq. 8.4).

Equations (8.3) and (8.4) imply that, for a star with $M < M_{Ch}$ that contracts quasi-statically, T_c increases as $\rho_c^{1/3}$ until the electrons become degenerate. Then a maximum temperature is reached, and subsequently the star cools at a constant density when degenerate electrons provide the pressure. The schematic evolution tracks for 0.1 and $1.0 M_\odot$ given in Fig. 8.2 show this behaviour. This can be compared to eq. (7.41) for homologous contraction (Sec. 7.4.3), which indicates that the slope of an evolution track in the $\log T - \log \rho$ plane is equal to $(\frac{4}{3} - \chi_\rho)/\chi_T$. This equals $\frac{1}{3}$ for an ideal gas, but changes sign and becomes negative once $\chi_\rho > \frac{4}{3}$. When degeneracy is almost complete, $\chi_\rho = \frac{5}{3}$ and $\chi_T \rightarrow 0$ such that the slope approaches infinity. The maximum temperature is reached when the

¹It is easy to show for yourself that the evolution track for a star in which radiation pressure dominates would have the same slope of $\frac{1}{3}$ in the $\log T, \log \rho$ plane. However, such stars are very close to dynamical instability.

ideal gas pressure and degenerate electron pressure are about equal, each contributing about half of the total pressure. Combining eqs. (8.3) and (8.4) then implies that the maximum central temperature reached increases with stellar mass as (see Exercise 8.2)

$$T_{c,\max} = \frac{C^2 G^2}{4\mathcal{R} K_{\text{NR}}} \mu \mu_{\text{e}}^{5/3} M^{4/3}. \quad (8.5)$$

For $M > M_{\text{Ch}}$, the tracks of contracting stars miss the degenerate region of the T - ρ plane, because at high density the boundary between ideal gas and degeneracy has the same slope as an evolution track. The pressure remains dominated by an ideal gas, and T_c keeps increasing like $\rho_c^{1/3}$ to very high values ($> 10^{10}$ K). This behaviour is shown by the schematic tracks for 10 and 100 M_{\odot} .

8.2 Nuclear burning regions and limits to stellar masses

We found that stars with $M < M_{\text{Ch}}$ reach a maximum temperature, the value of which increases with mass. This means that only gas spheres above a certain mass limit will reach temperatures sufficiently high for nuclear burning. The nuclear energy generation rate is a sensitive function of the temperature, which can be written as

$$\epsilon_{\text{nuc}} = \epsilon_0 \rho^{\lambda} T^{\nu} \quad (8.6)$$

where for most nuclear reactions (those involving two nuclei) $\lambda = 1$, while ν depends mainly on the masses and charges of the nuclei involved and usually $\nu \gg 1$. For H-burning by the pp-chain, $\nu \approx 4$ and for the CNO-cycle which dominates at somewhat higher temperature, $\nu \approx 18$. For He-burning by the 3α reaction, $\nu \sim 40$ (and $\lambda = 2$ because three particles are involved). For C-burning and O-burning reactions ν is even larger. As discussed in Chapter 6, the consequences of this strong temperature sensitivity are that

- each nuclear reaction takes place at a particular, nearly constant temperature, and
- nuclear burning cycles of subsequent heavier elements are well separated in temperature

As a star contracts and heats up, nuclear burning becomes important when the energy generated, $L_{\text{nuc}} = \int \epsilon_{\text{nuc}} dm$, becomes comparable to the energy radiated away from the surface, L . From this moment on, the star can compensate its surface energy loss by nuclear energy generation: it comes into *thermal equilibrium*. The first nuclear fuel to be ignited is hydrogen, at $T_c \sim 10^7$ K. From the homology relation (7.38) we expect that the central temperature at which hydrogen fusion stabilizes should depend on the mass approximately as

$$T_c = T_{c,\odot} (M/M_{\odot})^{4/(\nu+3)} \quad (8.7)$$

where $T_{c,\odot} \approx 1.5 \times 10^7$ K, for a composition like that of the Sun ($\mu = \mu_{\odot}$). We can estimate the minimum mass required for hydrogen burning by comparing this temperature to the maximum central temperature reached by a gas sphere of mass M , eq. (8.5). By doing this (and taking $C = 0.48$ for an $n = 1.5$ polytrope) we find a minimum mass for hydrogen burning of $0.15 M_{\odot}$.

Detailed calculations reveal that the minimum mass for the ignition of hydrogen in protostars is about 2 times smaller than this simple estimate, $M_{\text{min}} = 0.08 M_{\odot}$. Less massive objects become partially degenerate before the required temperature is reached and continue to contract and cool without ever burning hydrogen. Such objects are not stars according to our definition (Chapter 1) but are known as *brown dwarfs*.

We have seen earlier that the contribution of radiation pressure increases with mass, and becomes dominant for $M \gtrsim 100 M_{\odot}$. A gas dominated by radiation pressure has an adiabatic index $\gamma_{\text{ad}} = \frac{4}{3}$,

which means that hydrostatic equilibrium in such stars becomes marginally unstable (see Sec. 7.5.1). Therefore stars much more massive than $100 M_{\odot}$ should be very unstable, and indeed none are known to exist (while those with $M > 50 M_{\odot}$ indeed show signs of being close to instability, e.g. they lose mass very readily).

Hence stars are limited to a rather narrow mass range of $\sim 0.1 M_{\odot}$ to $\sim 100 M_{\odot}$. The lower limit is set by the minimum temperature required for nuclear burning, and the upper limit by the requirement of dynamical stability.

8.2.1 Overall picture of stellar evolution and nuclear burning cycles

As a consequence of the virial theorem, a self-gravitating sphere composed of ideal gas in HE must contract and heat up as it radiates energy from the surface. The energy loss occurs at a rate

$$L = -\dot{E}_{\text{tot}} = \dot{E}_{\text{in}} = -\frac{1}{2}\dot{E}_{\text{gr}} \approx \frac{E_{\text{gr}}}{\tau_{\text{KH}}} \quad (8.8)$$

This is the case for protostars that have formed out of an interstellar gas cloud. Their evolution, i.e. overall contraction, takes place on a thermal timescale τ_{KH} . As the protostar contracts and heats up and its central temperature approaches 10^7 K, the nuclear energy generation rate (which is at first negligible) increases rapidly in the centre, until the burning rate matches the energy loss from the surface:

$$L = -\dot{E}_{\text{nuc}} \approx \frac{E_{\text{nuc}}}{\tau_{\text{nuc}}} \quad (8.9)$$

At this point, contraction stops and T_c and ρ_c remain approximately constant, at the values needed for hydrogen burning. The stellar centre occupies the same place in the T_c - ρ_c diagram for about a nuclear timescale τ_{nuc} . Remember that for a star of a certain mass, L is essentially determined by the opacity, i.e. by how efficiently the energy can be transported outwards.

When H is exhausted in the core – which now consists of He and has a mass typically $\sim 10\%$ of the total mass M – this helium core resumes its contraction. Meanwhile the layers around it expand. This constitutes a large deviation from homology and relation (8.1) no longer applies to the whole star. However the core itself still contracts more or less homologously, while the weight of the envelope decreases as a result of its expansion. Therefore relation (8.1) remains approximately valid for the *core* of the star, i.e. if we replace M by the core mass M_c . The core continues to contract and heat up at a pace set by its own thermal timescale,

$$L_{\text{core}} \approx \dot{E}_{\text{in,core}} \approx -\frac{1}{2}\dot{E}_{\text{gr,core}} \approx \frac{E_{\text{gr,core}}}{\tau_{\text{KH,core}}} \quad (8.10)$$

as long as the gas conditions remain ideal. It is now the He core mass, rather than the total mass of the star, that determines the further evolution.

Arguments similar to those used for deriving the minimum mass for H-burning lead to the existence a minimum (core) mass for He-ignition, This is schematically depicted in Fig. 8.3, which suggests that this minimum mass is larger than $1 M_{\odot}$. However, the schematic tracks in Fig. 8.3 have been calculated for a fixed composition $X = 0.7$, $Z = 0.02$, which is clearly no longer the valid since the core is composed of helium. You may verify that a He-rich composition increases the maximum central temperature reached for a certain mass (eq. 8.5). Detailed calculations put the minimum mass for He-ignition at $\approx 0.3 M_{\odot}$. Stars with a core mass larger than this value ignite He in the centre when $T_c \approx 10^8$ K, which stops further contraction while the energy radiated away can be supplied

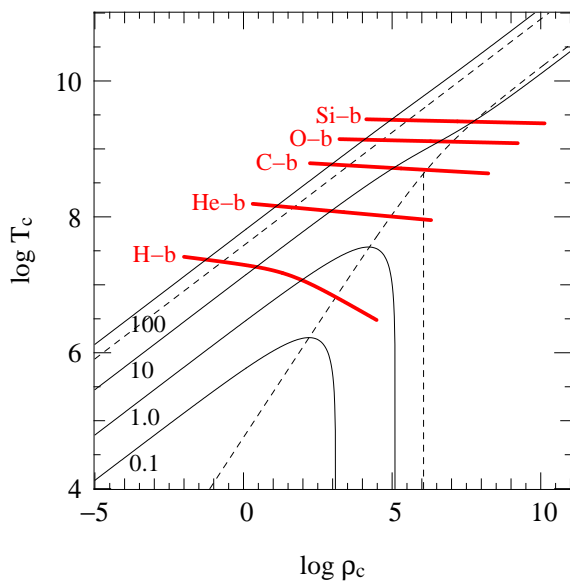


Figure 8.3. The same schematic evolution tracks as in Fig. 8.2, together with the approximate regions in the $\log T_c - \log \rho_c$ plane where nuclear burning stages occur.

by He-burning reactions. This can go on for a length of time equal to the nuclear timescale of He burning, which is about 0.1 times that of H burning. In stars with a He core mass $< 0.3 M_\odot$ the core becomes degenerate before reaching $T_c = 10^8$ K, and in the absence of a surrounding envelope it would cool to become a white dwarf composed of helium, as suggested by Fig. 8.3. (In practice, however, H-burning in a shell around the core keeps the core hot and when M_c has grown to $\approx 0.5 M_\odot$ He ignites in a degenerate flash.)

After the exhaustion of He in the core, the core again resumes its contraction on a thermal timescale, until the next fuel can be ignited. Following a similar line of reasoning the minimum (core) mass for C-burning, which requires $T \approx 5 \times 10^8$ K, is $\approx 1.1 M_\odot$. Less massive cores are destined to never ignite carbon but to become degenerate and cool as CO white dwarfs. The minimum core mass required for the next stage, Ne-burning, turns out to be $\approx M_{\text{Ch}}$. Stars that develop cores with $M_c > M_{\text{Ch}}$ therefore also undergo all subsequent nuclear burning stages (Ne-, O- and Si-burning) because they never become degenerate and continue to contract and heat after each burning phase. Eventually they develop a core consisting of Fe, from which no further nuclear energy can be squeezed. The Fe core must collapse in a cataclysmic event (a supernova or a gamma-ray burst) and become a neutron star or black hole.

The alternation of gravitational contraction and nuclear burning stages is summarized in Table 8.1, together with the corresponding minimum masses and characteristic temperatures and energies. The schematic picture presented in Fig. 8.3 of the evolution of stars of different masses in the $T-\rho$ diagram can be compared to Fig. 8.4, which shows the results of detailed calculations for various masses.

To summarize, we have obtained the following picture. Nuclear burning cycles can be seen as long-lived but temporary interruptions of the inexorable contraction of a star (or at least its core) under the influence of gravity. This contraction is dictated by the virial theorem, and a result of the fact that stars are hot and lose energy by radiation. If the core mass is less than the Chandrasekhar mass, then the contraction can eventually be stopped (after one or more nuclear cycles) when electron degeneracy supplies the pressure needed to withstand gravity. However if the core mass exceeds the Chandrasekhar mass, then degeneracy pressure is not enough and contraction, interrupted by nuclear burning cycles, must continue at least until nuclear densities are reached.

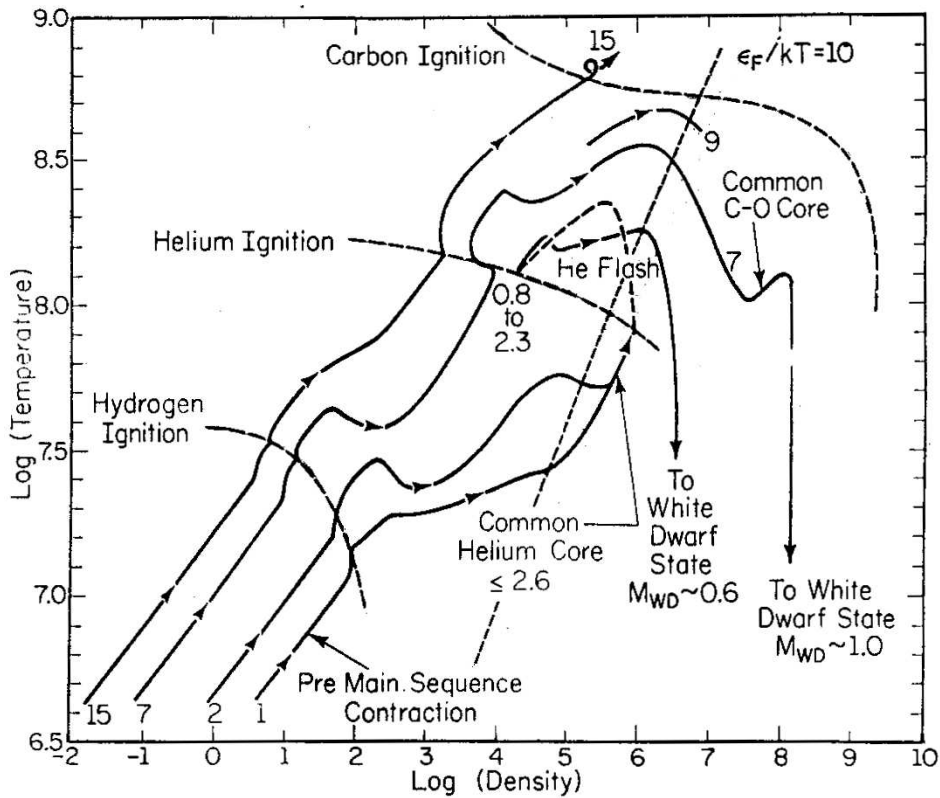


Figure 8.4. Detailed evolution tracks in the $\log \rho_c - \log T_c$ plane for masses between 1 and $15 M_{\odot}$. The initial slope of each track (labelled pre-main sequence contraction) is equal to $\frac{1}{3}$ as expected from our simple analysis. When the H-ignition line is reached wiggles appear in the tracks, because the contraction is then no longer strictly homologous. A stronger deviation from homologous contraction occurs at the end of H-burning, because only the core contracts while the outer layers expand. Accordingly, the tracks shift to higher density appropriate for their smaller (core) mass. These deviations from homology occur at each nuclear burning stage. Consistent with our expectations, the most massive star ($15 M_{\odot}$) reaches C-ignition and keeps evolving to higher T and ρ . The core of the $7 M_{\odot}$ star crosses the electron degeneracy border (indicated by $\epsilon_F/kT = 10$) before the C-ignition temperature is reached and becomes a C-O white dwarf. The lowest-mass tracks (1 and $2 M_{\odot}$) cross the degeneracy border before He-ignition because their cores are less massive than $0.3 M_{\odot}$. Based on our simple analysis we would expect them to cool and become He white dwarfs; however, their degenerate He cores keep getting more massive and hotter due to H-shell burning. They finally do ignite helium in an unstable manner, the so-called He flash.

Suggestions for further reading

The schematic picture of stellar evolution presented above is very nicely explained in Chapter 7 of PRIALNIK, which was one of the sources of inspiration for this chapter. The contents are only briefly covered by MAEDER in Sec. 3.4, and are somewhat scattered throughout KIPPENHAHN & WEIGERT, see sections 28.1, 33.1, 33.4 and 34.1.

Table 8.1. Characteristics of subsequent gravitational contraction and nuclear burning stages. Column (3) gives the total gravitational energy emitted per nucleon since the beginning, and column (5) the total nuclear energy emitted per nucleon since the beginning. Column (6) gives the minimum mass required to ignite a certain burning stage (column 4). The last two columns give the fraction of energy emitted as photons and neutrinos, respectively.

phase	T (10^6 K)	total E_{gr}/n	main reactions	total E_{nuc}/n	M_{min}	γ (%)	ν (%)
grav.	$0 \rightarrow 10$	~ 1 keV/n				100	
nucl.	$10 \rightarrow 30$		${}^1\text{H} \rightarrow {}^4\text{He}$	6.7 MeV/n	$0.08 M_{\odot}$	~ 95	~ 5
grav.	$30 \rightarrow 100$	~ 10 keV/n				100	
nucl.	$100 \rightarrow 300$		${}^4\text{He} \rightarrow {}^{12}\text{C}, {}^{16}\text{O}$	≈ 7.4 MeV/n	$0.3 M_{\odot}$	~ 100	~ 0
grav.	$300 \rightarrow 700$	~ 100 keV/n				~ 50	~ 50
nucl.	$700 \rightarrow 1000$		${}^{12}\text{C} \rightarrow \text{Mg, Ne}$	≈ 7.7 MeV/n	$1.1 M_{\odot}$	~ 0	~ 100
grav.	$1000 \rightarrow 1500$	~ 150 keV/n					~ 100
nucl.	$1500 \rightarrow 2000$		${}^{16}\text{O} \rightarrow \text{S, Si}$	≈ 8.0 MeV/n	$1.4 M_{\odot}$		~ 100
grav.	$2000 \rightarrow 5000$	~ 400 keV/n	$\text{Si} \rightarrow \dots \rightarrow \text{Fe}$	≈ 8.4 MeV/n			~ 100

Exercises

8.1 Homologous contraction (1)

- Explain in your own words what *homologous contraction* means.
- A real star does not evolve homologously. Can you give a specific example? [Think of core versus envelope]
- Fig. 8.3 shows the central temperature versus the central density for schematic evolution tracks assuming homologous contraction. Explain qualitatively what we can learn from this figure (nuclear burning cycles, difference between a $1 M_{\odot}$ and a $10 M_{\odot}$ star, ...)
- Fig. 8.4 shows the same diagram with evolution tracks from detailed (i.e. more realistic) models. Which aspects were already present in the schematic evolution tracks? When and where do they differ?

8.2 Homologous contraction (2)

In this question you will derive the equations that are plotted in Figure 8.2b.

- Use the homology relations for P and ρ to derive eq. (8.1),

$$P_c = CGM^{2/3} \rho_c^{4/3}$$

To see what happens qualitatively to a contracting star of given mass M , the total gas pressure can be approximated roughly by:

$$P \approx P_{\text{id}} + P_{\text{deg}} = \frac{\mathcal{R}}{\mu} \rho T + K \left(\frac{\rho}{\mu_e} \right)^{\gamma} \quad (8.11)$$

where γ varies between $\frac{5}{3}$ (non-relativistic) and $\frac{4}{3}$ (extremely relativistic).

- Combine this equation, for the case of NR degeneracy, with the central pressure of a contracting star in hydrostatic equilibrium (eq. 8.1, assuming $C \approx 0.5$) in order to find how T_c depends on ρ_c .
- Derive an expression for the maximum central temperature reached by a star of mass M .

8.3 Application: minimum core mass for helium burning

Consider a star that consists completely of helium. Compute an estimate for the minimum mass for which such a star can ignite helium, as follows.

- Assume that helium ignites at $T_c = 10^8$ K.
- Assume that the critical mass can be determined by the condition that the ideal gas pressure and the electron degeneracy pressure are equally important in the star at the moment of ignition.
- Use the homology relations for the pressure and the density. Assume that $P_{c,\odot} = 10^{17}$ g cm⁻¹ s⁻² and $\rho_{c,\odot} = 60$ g cm⁻³.